Optimal Coupling of NbN HEB THz Mixers to Cryogenic HEMT IF Low-Noise Amplifiers

Fernando Rodriguez-Morales, Sigfrid Yngvesson, Dazhen Gu, Eyal Gerecht,
Niklas Wadefalk, Ric Zannoni, and John Nicholson

***Abstract*— We are proposing a general approach to find the optimal coupling conditions between a NbN HEB mixer and its corresponding HEMT IF amplifier. We present our progress towards the development of suitable models for the analysis of the mixer/LNA sub-system in HEB terahertz down-converters. Our modeling approach takes into account parasitic reactances from the antenna and coplanar waveguide (CPW) structures, wire-bonds, the effect of the biasing networks, etc. We discuss the implementation of a lumped-element matching network designed based on the optimal matching considerations, which can in principle be integrated into an MMIC LNA. Finally, we suggest packaging schemes to further reduce the size of the integrated receivers in order to accommodate a larger number of pixels in a focal plane array.**

***Index Terms*— HEB mixers, integrated terahertz receivers, MMIC low-noise amplifiers, HEB IF impedance.**

I. Introduction

HOT ELECTRON BOLOMETRIC (HEB) mixer technology is gradually reaching maturity, and a wide range of new applications is presently emerging. The technical interest in HEB receiver systems is being shifted towards the development of imaging arrays for surveillance and biomedical applications [1], in addition to the more traditional radio-astronomy receivers. In such systems, it is essential that the HEB mixers are placed in close proximity with the intermediate frequency (IF) amplifiers, in order to realize a small size array while achieving the minimum inter-element spacing required for enhanced spatial resolution. The integration of HEB mixers with MMIC IF amplifiers has been addressed in previous papers by the authors [2], [3]. These receivers have demonstrated near-quantum limited noise performance (in the range of $10-20\times hf/k$) and very wide effective IF bandwidths (up to 5 GHz).

In these detectors, the effective bandwidth is predominantly constrained by a non-trivial relationship between the mixer and the LNA. Modeling this interaction both accurately and rigourously has been a major challenge, particularly because presently available models for HEBs lack completeness [4], [5]. Furthermore, the noise parameters of the amplifier change as the IF output impedance of the phonon-cooled mixer varies for different operating conditions [6].

In order to better understand this mutual coupling and thereby optimize the performance of the integrated down-converters, it becomes necessary to develop suitable models that will be useful in deriving optimum design guidelines for an HEB-HEMT system, as was done by Weinreb for the SIS-HEMT case [7]. This paper presents our progress towards the development of such models. We start by discussing methodologies to accurately determine the HEB IF output impedance for different dynamic conditions, using Automatic Network Analyzer (ANA) measurements. Next, we discuss different alternatives to accomplish the optimal coupling of the HEB mixer with the IF amplifier. Finally, we propose different packaging schemes in order to use the optimized receivers as the basis for compact arrays with denser element population.

F. Rodriguez-Morales, K.S. Yngvesson, D. Gu, E. Gerecht, R. Zannoni, and J. Nicholson are with the University of Massachusetts at Amherst, Amherst, MA 01002 USA (e-mail: frodrigu@ecs.umass.edu); N. Wadefalk is with Chalmers University of Technology, SE-412 96, Göteborg, Sweden.

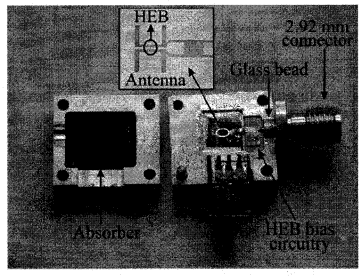

Fig. 1. Inside view of the fixture employed for HEB impedance characterization. The antenna shown in this picture corresponds to a twin-slot design (used for 750 GHz and 1.2 THz, respectively). A log-periodic antenna structure was used for 1.6 THz

II. IF Small Signal Impedance Measurements

We have obtained the small signal IF impedance Z of various receiver devices operating under different dynamic conditions. The magnitude and phase of the scattering parameter S_{11} have been measured under the presence of LO laser illumination and dc-bias, using an Agilent E5071B ANA. The measurements have been completed on three separate devices for three different LO frequencies: 750 GHz, 1.2 THz, and 1.6 THz. For the 750 GHz and 1.2 THz experiments we used twin-slot antennas integrated with 4 μm $\times$.5 μm HEB devices. The device under test (DUT) for 1.6 THz had dimensions 4 μm $\times$.6 μm and was integrated with a self-complementary log-periodic antenna. The IF range used was 300 kHz to 5 GHz, which covers the typical IF bandwidth for most phonon-cooled NbN HEB mixers. The measurements required an initial one-port short-open-load (SOL) calibration inside the cryostat, in contrast to the TRL calibration employed in [8]. The calibration was done by putting each of the standards into the dewar in three consecutive thermal cycles

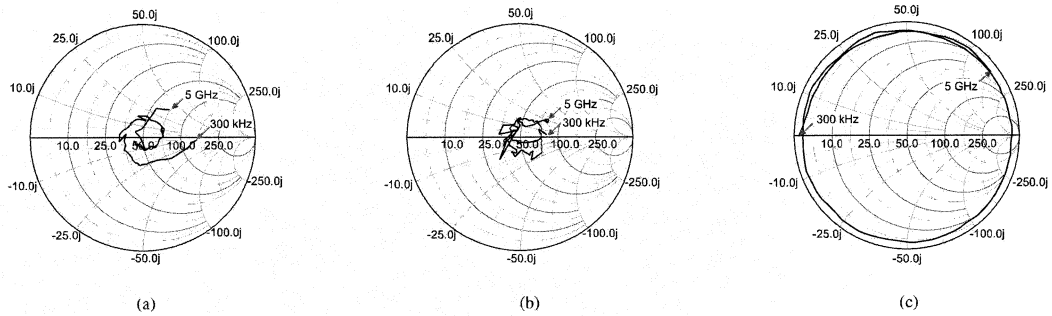

Fig. 2. Examples of Smith chart plots of the parameter S_{11} obtained for two different devices under different biasing (optimum) conditions: (a) 750 GHz LO for 0.5 mV, 39 μA; (b) 1.6 THz LO for 0.5 mV, 46 μA; and (c) superconducting short used as reflect standard for de-embedding.

and measuring the corresponding S_{11} using the ANA. The power level from the network analyzer was -48 dBm. The specimens were mounted on a special fixture (shown in Fig 1), which includes a broadband biasing circuit constructed from quartz wire-bondable resistors.

The stability properties of HEB devices change with different biasing networks [9] and the source impedance presented to the LNA is slightly affected by the parasitics introduced by this circuit. Therefore it is important to complete these measurements with the same biasing scheme as will be used in the actual receivers. The use of resistors with a high self-resonant frequency (SRF) facilitates removing the effect of the dc-network from the measurement via de-embedding, which is convenient for device modeling.

A. Raw Reflection Coefficient

Fig. 2 shows examples of Smith chart plots of the reflection coefficient for two of the measured devices, as obtained with the network analyzer. These are the actual source impedances seen by the low-noise amplifier at the given operating points, including parasitic reactances in the circuit derived from the antenna structure, wire-bonds, transmission line transitions, etc. Though the HEB impedance determines the main contribution to the total input reflection coefficient of the LNA, parasitic reactances in the circuit should not be neglected when designing the appropriate input matching network for minimum noise.

B. HEB Impedance De-Embedding

The HEB IF small signal was carefully de-embedded from the the measured reflection coefficient (S_{11}). The preceding SOL cryogenic calibration was used in combination with the S-parameters of two measured known loads (superconducting and normal state of the bolometer, respectively) to obtain a circuit model for the fixture parasitics. Computer simulations were then used to predict the response of an open circuit in place of the HEB device. A one-port error model was then obtained by means of the above new "standards". The error model accounts for the directivity error e_{00}, the source match error e_{11}, as well as the reflection tracking error (e_{10} e_{01}). Using these error terms, the HEB IF small signal impedance

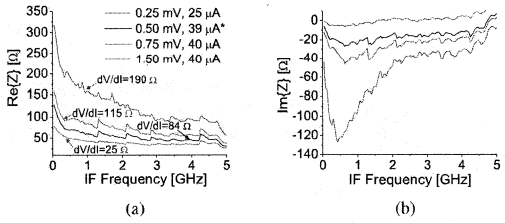

Fig. 3. De-embedded impedance for an HEB receiver device operating at 750 GHz: (a) Real part, and (b) Imaginary part.

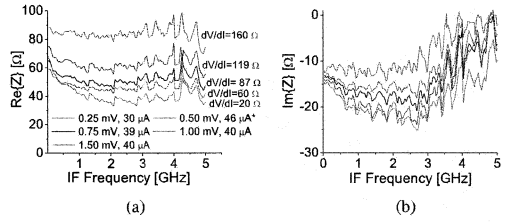

Fig. 4. De-embedded impedance for an HEB receiver device operating at 1.6 THz: (a) Real part, and (b) Imaginary part.

can be accurately extracted from the microwave reflection measurements. Fig. 3 and Fig. 4 show the de-embedded results for two of the measured devices. The * symbol indicates the optimum conditions for minimum receiver noise, which were found after subsequent noise measurements were performed on these devices.

C. Discussion

There is a strong correlation between the numerical value of the dynamic differential resistance obtained from the dc IV curves, dV/dI, and the real part of the impedance, $\mathrm{Re}\{Z\}$. This holds true specially for IF frequencies between 1 to 5 GHz, where the impedance is also dominated by its real part. As expected, the reactive part of Z is purely capacitive over the entire frequency range.

The corresponding dV/dI for different operating points appears in Tables I and II. These tables also include a summary

TABLE I
SUMMARIZED RESULTS FOR Z AND dV/dI AT 750 GHz.

Operating Point	Re{Z}[Ohms] 1GHz/4GHz	Im{Z}[Ohms] 1GHz/4GHz	dV/dI [Ohms]
0.25 mV, 25 μA	42/35	-4/0	24
0.50 mV, 39 μA*	60/42	-23/-11	84
0.75 mV, 40 μA	85/58	-39/-18	114
1.50 mV, 40 μA	158/95	-93/-31	190

TABLE II
SUMMARIZED RESULTS FOR Z AND dV/dI AT 1.6 THz.

Operating Point	Re{Z}[Ohms] 1GHz/4GHz	Im{Z}[Ohms] 1GHz/4GHz	dV/dI [Ohms]
0.25 mV, 30 μA	42/42	-22/-11.0	16
0.50 mV, 46 μA*	46/52	-19/-10.4	60
0.75 mV, 39 μA	50/58	-17/-4.5	88
1.00 mV, 40 μA	61/76	-15/-2.8	119
1.50 mV, 45 μA	82/95	-12/-1.5	160

of the results presented previously in Figs. 3 and 4. Fig. 5 displays the ratio between Re{Z} and dV/dI ($\wp$) throughout the important IF range, which has been calculated to emphasize the above correlation. This ratio remains in the order of 0.5–0.8 for biasing points near the optimum. For the 750 GHz device the measurements are in fair qualitative agreement with the so-called *standard model* (uniform bolometer heating) [8], [10], while being substantially different for 1.2 THz (not shown) and 1.6 THz. It is noteworthy that 750 GHz is below the bandgap frequency of the superconductor, which may partly explain this discrepancy. More measurements need to be performed at 1.0 THz and above in order to resolve the deviation of these results from the standard model and to better understand the dependency of Z with respect to frequency, biasing conditions, and device parameters. To date, we have developed the capability for accurately determining the reflection coefficient seen by the IF amplifier as well as the contribution of the HEB IF output impedance alone.

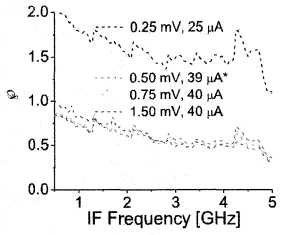

(a)

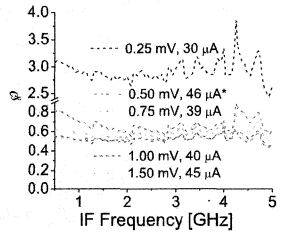

(b)

Fig. 5. Ratio between the real part of Z and the differential dynamic resistance for different operating points for: (a) 750 GHz LO; (b) 1.6 THz LO. For the 750 GHz LO and low IF frequencies $\wp$ is nearly unity, in agreement with the standard model.

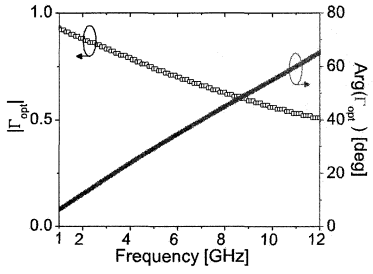

Fig. 6. Simulated optimum input reflection coefficient Γ_{opt} for our previously developed MMIC LNA (without any matching network).

III. HEB-LNA Coupling

In order to realize the best trade-off between low-noise figure and wide bandwidth, the coupling between the HEB mixer output and the HEMT LNA input needs to be studied. This analysis evidently requires the knowledge of the impedance presented by the HEB and surrounding circuitry, which was the center of our discussion in the previous Section. Once this source impedance is known through either modeling or measurements, an appropriate input matching network (IMN) can be designed to transform the HEB IF output impedance into the intended optimum source impedance Z_{opt} required by the LNA (Fig. 6). Since the input impedance of a HEMT-based amplifier is mainly dominated by the gate-to-source capacitive reactance of the first transistor stage, the IMN should behave as a series inductor. Such IMN has already been successfully implemented by our group in the form of a multi-section microstrip transformer but other alternatives are being investigated. The use of a lumped-element matching network or wire-bonds as inductive elements as proposed in [11] (Fig. 7), will help further reduce the size of the HEB down-converter while maintaining the low-noise characteristics.

IV. New Array Packaging Schemes

Our group has previously demonstrated the first heterodyne focal plane array receiver unit designed for operation at terahertz frequencies. This FPA module uses integrated receiver elements arranged in a fly's eye configuration [2]. The number of elements in such array can be augmented straightforwardly up to $2 \times n$. Nevertheless, for a larger FPA this approach would lack adequate space for complete IF and DC-bias circuits and will present potential difficulties in thermal power dissipation. To overcome these problems, future extensions to our work include investigating alternative packaging schemes

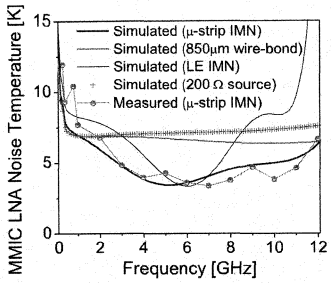

Fig. 7. Noise performance variation of our previously developed MMIC LNA IF amplifier for different input matching circuits. The + symbol corresponds to an hypothetical case in which the HEB IF impedance is purely real and equal to 200 Ω.

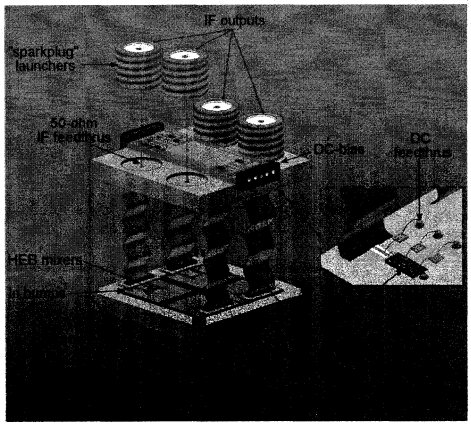

Fig. 8. The proposed configuration for the prototype 2 x 2 element terahertz heterodyne focal plane array; (inset) Placement of IF MMIC LNAs.

to integrate all the receiver elements more compactly, using a three-dimensional configuration. An illustration of one such prototype FPA is presented in Fig. 8.

An important feature of this layout is the incorporation of polyimide (Kapton) ribbons with CPW transmission lines designed to carry the IF and dc-biasing signals. These Kapton lines minimize the thermal conduction from the HEB board (which is at 4 K) to the IF board in Fig. 8. The IF board containing the MMIC LNAs can be cooled to a higher temperature (15 K to 20 K) without affecting the noise performance of the chips. We have started investigating the properties of the flexible CPWs in order to achieve highly integrated FPAs. As a first step we have performed full electromagnetic analysis of the response of a CPW transformer fabricated on flexible substrate (ϵ_r=3.5). The circuit has been designed as the IMN for our previously developed MMIC LNA. The simulations include the effect of the wire bonds used to contact the HEB and LNA chips at either end of the transformer. The performance of this transformer is comparable with that of the microstrip implementation over the entire band of interest.

V. Conclusion

Highly integrated receiver modules with high functionality can be very attractive for imaging and other terahertz applications. We are addressing the modeling of the optimal coupling between HEB mixers integrated with HEMT IF amplifiers.

As a first step, we have developed de-embedding routines to obtain the HEB small signal impedance as a function of IF frequency and under various operating conditions. We have discussed the correlation between the real part of the impedance and the dynamic resistance of the mixer. We have also been able to accurately determine the source impedance presented to the LNA by the HEB chip and surrounding circuitry. We have proposed various alternatives for an optimal input matching circuit for the LNA, which can be integrated into the amplifier itself. Lastly, we have started the investigation of new packaging schemes for array receivers. These new schemes include the development of highly integrated modules connected in a three-dimensional configuration using Kapton CPW lines. These HEB down-converters will be the basis of large FPAs for the next-generation terahertz imagers.

Acknowledgment

We would like to thank Dr. S. Weinreb for kindly supplying the MMIC chips used in our integrated receivers.

References

[1] D. Gu, E. Gerecht, F. Rodriguez-Morales, and S. Yngvesson, "A Two Dimensional Terahertz Imaging System Using Hot Electron Bolometer Technology." this symposium.

[2] F. Rodriguez-Morales, K. S. Yngvesson, E. Gerecht, N. Wadefalk, J. Nicholson, D. Gu, X. Zhao, T. Goyette, and J. Waldman, "A Terahertz Focal Plane Array Using HEB Superconducting Mixers and MMIC IF Amplifiers," *IEEE Microw. Wireless Comp. Lett.*, vol. 15, no. 4, pp. 199–201, Apr. 2005.

[3] F. Rodriguez-Morales, S. Yngvesson, R. Zannoni, E. Gerecht, D.Gu, N. Wadefalk, and J.Nicholson, "Development of Integrated HEB/MMIC Receivers for Near-Range Terahertz Imaging," *IEEE Trans. Microw. Theory Tech.*, vol. 54, no. 6, Jun. 2006.

[4] H. Ekstroem, B. Karasik, E. Kollberg, and S. Yngvesson, "Conversion Gain and Noise of Niobium Superconducting Hot-Electron Mixers," *IEEE Trans. Microw. Theory Tech.*, vol. 43, no. 4, pp. 938–947, Apr. 1995.

[5] H. Merkel, P. Khosropanah, P. Yagoubov, and E. Kollberg, "A Hot-Spot Mixer Model for Phonon-Cooled NbN Hot Electron Bolometric Mixers," *IEEE Trans. on Appl. Superconduct.*, vol. 9, no. 2, pp. 4201–4204, Jun. 1999.

[6] R. Hu and S. Weinreb, "A Novel Wide-Band Noise Parameter Measurement Method and its Cryogenic Application," *IEEE Trans. Microw. Theory Tech.*, vol. 52, no. 5, pp. 1498–1507, May 2004.

[7] S. Weinreb, "SIS Mixer to HEMT Amplifier Optimum Coupling Network," *IEEE Trans. Microw. Theory Tech.*, vol. 35, no. 11, pp. 1067–1069, Nov. 1987.

[8] F. Rodriguez-Morales and K. S. Yngvesson, "Impedance and Bandwidth Characterization of NbN Hot Electron Bolometric Mixers," in *Proc. 14th Int. Symp. Space Terahertz Tech., Tucson, Az*, Apr. 2003, pp. 431–438.

[9] Y. Zhuang, "Linear and Nonlinear Characteristics of NbN Hot Electron Bolometer Devices," Ph.D. dissertation, University of Massachusetts Amherst, USA, 2002.

[10] J. Kooi, J. J. A. Baselmans, J. R. Gao, T. M. Klapwijk, M. Hajenius, P. Dieleman, A. Baryshev, and G. de Lange, "IF Impedance and Mixer Gain of Hot Electron Bolometers and the Perrin–Vanneste Two Temperature Model," this symposium.

[11] F. Rodriguez-Morales, E. Gerecht, D. Gu, R. Zannoni, S. Yngvesson, N. Wadefalk, and J. Nicholson, "Performance Improvement of Integrated HEB-MMIC Receivers for Multi-Pixel Terahertz Focal Plane Arrays." in *Proc. 16th Int. Symp. Space Terahertz Tech., Goteborg, Sweden*, May 2005, pp. 246–250.